Laser and Particle Beams (1997), *vol.* 15, *no.* 1, *pp.* 167–177
Printed in the United States of America

Coherence in Compton scattering at large angles[1]

By G. GIORDANO,* G. MATONE,*
A. LUCCIO,** AND L. MICELI**
*INFN, Laboratori Nazionali, 00044 Frascati, Italy
**Brookhaven National Laboratory, Upton, NY 11973

(Received 27 February 1995; Revised 14 August 1995; Accepted 30 March 1996)

Compton scattering of laser light by an electron beam at large angles, in particular at 90°, produces coherent hard radiation if the density of the electron beam is high enough. In this case, the intensity of the scattered radiation is greatly enhanced in a small cone around the forward direction of propagation of the electron beam. As an example, the production of 1-KeV coherent X rays is discussed.

1. Introduction

In head-on Compton scattering experiments, collective effects arise if the electron bunch length is shorter than the produced radiation wavelength (Luccio *et al.* 1990; Pellegrini 1992). In this case, all the electrons radiate in phase and the intensity of the scattered radiation becomes proportional to the square of the electron number.

For optical or shorter wavelengths, this is difficult to achieve in head-on collisions (Federici *et al.* 1980; Sandorfi *et al.* 1983), because typically electron pulses cannot be much shorter than a few millimeters. However, one can superimpose on the Gaussian electron distribution a small density modulation that acts as a spatial grating and can be sufficient to induce coherent contributions in Compton scattering, as it has been discussed earlier (Luccio *et al.* 1990).

In the present paper, we examine a different possibility where no density modulation is involved, but the electron and photon beams cross each other at a large angle. This considerably shortens the interaction region and, under particular circumstances, can lead to collective effects and to some degree of coherence of the Compton scattered photon beam.

It is important to observe that collective scattering and coherence in the scattered beam are not necessarily synonymous. If collective scattering occurs, in the electron reference frame (ERF) the intensity of the scattered beam increases with the square of the number of electrons involved. However, in the laboratory scattering angles and photon energies transform according to the Lorentz formulas and in many cases the resulting radiation loses its spatial coherence, measured by the phase correlation of photons separated at the detector by some distance of interest. A discussion of the collective emission of synchrotron radiation and its relation to the spatial coherence of the photon is given, for example, in Bénard and Rousseau (1974).

2. Scattering of a light wave by an electron bunch

Let us consider the process of scattering of a plane electromagnetic wave with a system of N_e electrons initially at rest. In the impulse approximation, the total electromagnetic field observed at a point $\mathbf{r}$ at a large distance from the source is given by (Lipkin 1987)

[1]Work done in part under the auspices of the U.S. Department of Energy.

 0263-0346/97 $11.00 + .10

$$\mathbf{E}_T = \sum_{n=1}^{N_e} \mathbf{E}_n = \mathbf{E} \sum_{n=1}^{N_e} e^{i\mathbf{q}\cdot\mathbf{r}_n}, \tag{1}$$

where $\mathbf{E}_n$ is the amplitude radiated by the single scatterer at the position $\mathbf{r}_n$, and the momentum transfer $\mathbf{q}$ is

$$\mathbf{q} = \mathbf{k} - \mathbf{k}'. \tag{2}$$

$\mathbf{k},\mathbf{k}'$ being the vector momentum of the incoming and outgoing photon, respectively. Equation (1) shows that the intensity $|\mathbf{E}_T|^2$ of the radiation obtained from the ensemble of N_e electrons is enhanced with respect to the intensity due to the single electron by the square of the charge form factor of the electron distribution (Jackson 1975)

$$|F(\mathbf{q})|^2 = \left| \sum_{n=1}^{N_e} e^{i\mathbf{q}\cdot\mathbf{r}_n} \right|^2 \tag{3}$$

Equation (1) implies that the scattering process collectively involves all the electrons so that, after the scattering, the single scatterer wave function does not change so much that its identity may be established by subsequent measurements. On the other hand, the electrons of a beam pulse are loosely bound to a particular site and the coupling of electrons on different sites with each other is negligible. Under these conditions, the momentum is randomly exchanged among all the scatterers and each electron is expected to share, on the average, the same fraction of the total. This means that the recoil momentum is essentially delivered to the electron bunch as a whole (Weber 1985). In this case and for large N_e, the mass of the scatterer becomes so large that the scattering can be considered as a pure Thomson process with no energy shift.

If the average spacing between adjacent electrons is much shorter than the wavelength corresponding to the momentum transfer $\mathbf{q}$, the enhancement form factor of equation (3) can be approximated by its integral expression

$$F(\mathbf{q}) = N_e \int_V \rho(\mathbf{r}) e^{i\mathbf{q}\cdot r} d\mathbf{r} \tag{4}$$

with the normalization condition

$$\int_V \rho(\mathbf{r}) d\mathbf{r} = 1. \tag{5}$$

When the momentum transfer is small enough that $\mathbf{q}\cdot\mathbf{r} \ll 1$ over the entire integration volume, $F(\mathbf{q}) \cong N_e$ and the cooperative effect of the N_e electrons generates a scattering intensity N_e^2 larger than from a single electron. Conversely, if the wavelength is much shorter than the average distance between the electrons in the bunch, the exponent of equation (4) can be large and widely different in value, with the consequence that $F(\mathbf{q})$ can rapidly fall toward zero. In this case, the integral approximation (4) fails because the scattering intensity can never drop below the incoherent contribution expected from the sum of the squares of the diagonal terms in equation (1). This is what happens in the usual backscattering experiments (Federici *et al.* 1980), where the enhancement form factor given by equation (4) vanishes, whereas the intensity expected from equation (1) yields a contribution proportional to N_e.

In general, if $I_0(\mathbf{q})$ is the Compton intensity per unit solid angle expected for a single electron, the total intensity generated by N_e electrons can be written as

$$I_N(\mathbf{q}) = I_0(\mathbf{q})|F(\mathbf{q})|^2 \tag{6}$$

and can never fall below the corresponding incoherent contribution

$$I_N^{inc}(\mathbf{q}) = N_e I_0(\mathbf{q}), \tag{7}$$

which represents the lowest value that the scattered intensity can have.

3. Electron and photon densities

Let us explicitly discuss the case of Compton scattering of photons by an electron beam, when the two beams interact at 90° in the laboratory (figure 1) (Luccio & Miceli 1994). This case has also been recently discussed in (Kim *et al.* 1992, 1994), where it has been proposed for the production of very short X-ray pulses. The aim of the present paper is to show that under these circumstances, when the electron density is high enough, collective effects arise.

For simplicity, assume to have a parallel beam pulse of N_e electrons traveling at a speed βc along the z-axis and having the density distribution described by

$$\rho_{e,L} = \frac{dN_e}{dx_L dy_L dz_L} = \frac{1}{(2\pi)^{3/2}} \frac{N_e}{\sigma_x \sigma_y \sigma_{z,L}} e^{-\frac{1}{2}\left(\frac{x_L^2}{\sigma_x^2} + \frac{y_L^2}{\sigma_y^2}\right) - \frac{(z_L - \beta c t_L)^2}{2\sigma_{z,L}^2}}. \tag{8}$$

The subscript L stands for LAB frame of reference and σ_x, σ_y, and $\sigma_{z,L}$ represent the electron bunch dimensions in the x and y (transverse) and z (longitudinal) directions.

A laser beam of wavelength λ_L propagates along the x-direction and is focused right on the electron trajectory, with an elliptical spot size of half axes η and ξ along the z- and y-axes, respectively (figure 1). The minimum values for η and ξ are limited by the momentum/position uncertainty principle and therefore the laser beam cannot be focused down to linear sizes less than $\lambda_L/2\pi$. In these extreme conditions of maximum focusing, the momentum distribution becomes substantially isotropic. Nonetheless, a Gaussian-like momentum distribution will always be assumed in the present paper.

The propagation law for Gaussian beams ensures that the positions and angles of the photon trajectories are completely noncorrelated at the waist location ($x_L = 0$). This allows the laser photon density (brightness) in the LAB frame to be factored in the following way

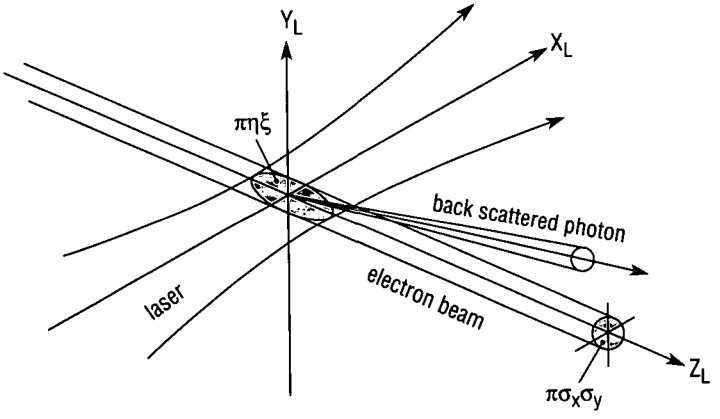

FIGURE 1. In the LAB frame, a laser beam of elliptical cross section $\pi\eta\xi$ interacts with an electron beam of cross section $\pi\sigma_x\sigma_y$ at 90°. Photons are scattered at a small angle to the direction of the e-beam.

$$\rho_{ph,L} = \frac{dN_{ph}}{dx_L dy_L dz_L d\ell dm} = \rho_{ph,0} h(\ell, m) e^{-\Gamma(x_L, y_L, z_L, \ell, m)}, \tag{9}$$

with the definitions

$$\begin{cases} \rho_{ph,0} = \dfrac{1}{\cos\theta_L} \dfrac{W}{2\pi c\hbar\omega\xi\eta\alpha}, \qquad h(\ell,m) = e^{-k_L^2(\ell^2\xi^2 + m^2\eta^2)}, \\ \alpha = \displaystyle\iint e^{-k_L^2(\ell^2\xi^2+m^2\eta^2)} d\ell\, dm = \frac{\pi}{k_L^2\xi\eta}, \\ \Gamma = \dfrac{1}{2\pi^2}(z_L - x_L \tan\theta_L \sin\phi_L)^2 + \dfrac{1}{2\xi^2}(y_L - x_L \tan\theta_L \cos\phi_L)^2, \end{cases} \tag{10}$$

and (all quantities defined in the LAB)

W = laser power [watt], c = speed of light,
$\hbar\omega$ = laser photon energy [joule],
$k_L = 2\pi/\lambda_L$ = laser photon wave vector [cm^{-1}],
$k_{x,L} = k_L \cos\theta_L$,
$k_{y,L} = k_L \ell$
$k_{z,L} = k_L m$,
$\ell = \sin\theta_L \cos\phi_L$, $m = \sin\theta_L \sin\phi_L$.

The angles of the incoming laser beam (in the LAB frame) θ_L, ϕ_L are defined in figure 2.

Because collective effects do not depend on the reference frame, we have chosen to perform the calculations in the ERF (variables with no subscripts), because in that frame the description of the process is simpler. This is due to the fact that in the ERF, the incoming and scattered wavelengths are equal. In the ERF, with the Lorentz transformations

$$x = x_L, \quad y = y_L, \quad z = \gamma(z_L - \beta c t_L), \quad ct = \gamma(ct_L - \beta z_L), \tag{11}$$

the electron density of equation (8) becomes

$$\rho_e(x,y,z) = \frac{dN_e}{dx\,dy\,dz} = \frac{N_e}{(2\pi)^{3/2}\sigma_x\sigma_y\sigma_z} e^{-\frac{1}{2}\left(\frac{x^2}{\sigma_x^2} + \frac{y^2}{\sigma_y^2} + \frac{z^2}{\sigma_z^2}\right)}. \tag{12}$$

In the absence of energy dispersion, this expression describes a completely stationary Gaussian pulse of length $\sigma_z = \gamma\sigma_{z,L}$.

Unfortunately, for the photon density the situation is much more complicated. Owing to the divergence, the monochromaticity is lost under the Lorentz transformation (equa-

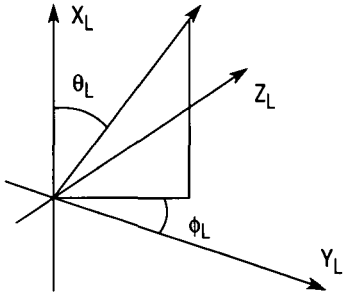

FIGURE 2. Definition of the angles of the incoming laser beam.

tion 11), and in the ERF frame the laser beam appears to be decomposed in a many-beam system with different frequency components.

It can be shown that, under the Lorentz transformation, equation (9) becomes

$$\rho_{ph}(x,y,z,\ell,m) = \frac{dN_{ph}}{dx\,dy\,dz\,d\ell\,dm} = \gamma(1-\beta m)\rho_{ph,L}. \tag{13}$$

Equations (10) and (13) state that for each value of ℓ and m in the LAB, the photon density in the ERF system appears to be concentrated in a cylindrical volume almost perpendicular to the y-z plane and sweeping across the pulse (equation 12) at the speed βc. But, because the Lorentz transformation acts differently on the spatial coordinates and the photon momenta, we obtain the interesting result that the photons inside each cylinder appear to travel in a direction almost parallel to the z-axis. In addition, because the Lorentz compression factor γ squeezes the cylinder along the z-direction, the laser light collides only against a tiny slice of the electron bunch.

The shape of this slice, specified by $e^{-\Gamma(x,y,z,\ell,m)}$, defines the volume of the electron pulse over which the integration of the form factor (equation 4) must be performed. For each specified value of ℓ and m, the form factor becomes

$$F(\mathbf{q},\ell,m) = \iiint_{-\infty,+\infty} \rho_e(x,y,z)e^{-\Gamma}e^{i\mathbf{q}\cdot\mathbf{r}}\,dx\,dy\,dz. \tag{14}$$

Because for the incoming (nonprimed quantities) and the outgoing (primed quantities) photons in the ERF is

$$\begin{cases} k_x = k_{x,L} \\ k_y = k_{y,L} \\ k_z = \gamma(k_{z,L} - \beta k_L) \\ k = \gamma(k_L - \beta k_{z,L}) \end{cases} \qquad \begin{cases} k'_x = k\cos\theta \\ k'_y = k\sin\theta\cos\phi \\ k'_z = k\sin\theta\sin\phi \end{cases} \tag{15}$$

the components of the momentum transfer of equation (2), in terms of the scattering angles θ and ϕ (defined in the ERF system as it has been done in figure 2 for the LAB system), are

$$\begin{cases} q_x = k_x - \gamma(k_L - \beta k_{z,L})\cos\theta \\ q_y = k_y - \gamma(k_L - \beta k_{z,L})\sin\theta\cos\phi \\ q_z = \gamma[k_{z,L} - \beta k_L - (k_L - \beta k_{z,L})\sin\theta\sin\phi]. \end{cases} \tag{16}$$

The integral of equation (14) is straightforward but not immediate. Following the definitions given in the Appendix, one obtains

$$F(\mathbf{q},\ell,m) = F_0 e^{-i\tilde{\mathbf{q}}\cdot\mathbf{r}_0}e^{-\frac{1}{4}\tilde{q}^2}, \tag{17}$$

where

$$F_0 \equiv F(\mathbf{q}=0) = \frac{1}{2^{3/2}}\frac{N_e}{\sigma_x\sigma_y\sigma_z}\frac{1}{uvf}e^{(r_0^2 - Ht^2)} \tag{18}$$

is the number of electrons contained in the illuminated volume.

Even though these electrons can only be a tiny fraction of the total number of electrons in the bunch, they backscatter in phase because they have been selected in a region of linear dimensions along the z-axis of the same order of the photon wavelength. Therefore,

depending upon the number of electrons that can be packed in one wavelength (i.e., the bunch density), the scattered intensity can be significantly higher than the usual incoherent contribution.

4. Scattered intensity

The total Compton intensity that results from the incoherent interaction between the two beams follows from the usual definition of the luminosity and can be written as

$$\frac{dI_N^{inc}}{d\ell dm} = c\sigma_{Th}\frac{d\Omega}{4\pi}\iiint_{-\infty,+\infty}\rho_e\rho_{ph}dx\,dy\,dz = c\sigma_{Th}\frac{d\Omega}{4\pi}\rho_{ph,0}\gamma(1-\beta m)h(\ell,m)F_0, \tag{19}$$

where σ_{Th} ($= 0.66\ 10^{-24}$ cm^2) is the Thomson scattering cross section. The same expression yields the total intensity generated by a single electron located at ($x = y = z = 0$)

$$\frac{dI_0}{d\ell dm} = c\sigma_{Th}\frac{d\Omega}{4\pi}\iiint_{-\infty,+\infty}\delta(0)\rho_{ph}dx\,dy\,dz = c\sigma_{Th}\frac{d\Omega}{4\pi}\rho_{ph,0}\gamma(1-\beta m)h(\ell,m)e^{-\frac{(\gamma\beta ct)^2}{2\eta^2}}. \tag{20}$$

It is interesting to notice that equation (20) can also be interpreted as an electron-to-photon conversion efficiency. Indeed, if the laser is not strongly focused on the electron beam (i.e., $\eta, \xi > \lambda_L/2\pi$), by integrating equation (20) over ℓ, m and time, one obtains

$$\Sigma_{e\to\gamma} \cong \frac{\sigma_{Th}}{\sqrt{2\pi}\beta c}\frac{W}{\hbar\omega\xi}, \tag{21}$$

which is the number of photons generated over the whole energy spectrum by one single electron that crosses a laser beam at 90°.

For a practical case, with a CO_2 laser, equation (21) yields an electron-to-photon efficiency given by

$$\Sigma_{e\to\gamma} = 4.1\times 10^{-16}\frac{W[\text{watt}]}{\xi[\text{cm}]}. \tag{22}$$

With $\xi = 25\ \mu$m and a laser power of 60 J/100 ps, this efficiency becomes $\approx 10\%$. This laser power is close to the record value already reported in the literature in single-shot operation (Ginzburg *et al.* 1983a). The impact that this observation has in the field of high energy colliders has been discussed at length in (Ginzburg *et al.* 1983b).

Finally, from equations (6) and (20), if we assume an isotropic differential cross section, the total intensity collectively generated by the N_e electrons of the bunch becomes

$$\frac{dI_N^{coh}}{d\ell dm} = \frac{c\sigma_{Th}}{4\pi}|F_0|^2\rho_{ph,0}\gamma(1-\beta m)h(\ell,m)\int_{4\pi}e^{-\frac{1}{2}\tilde{q}^2}d\Omega, \tag{23}$$

where the integration must be performed over the whole solid angle.

Both equations (19) and (23) represent two time pulses emerging from the interaction region with standard deviations that differ by $\sqrt{2}$, as they should. However, while the first photon pulse is isotropically diffused over the whole solid angle, the second is contained in a very narrow cone, whose axis direction depends on (ℓ, m). The ratio between coherent and incoherent flux at (ℓ, m) is

$$\Re(\ell,m) = \frac{dI_N^{coh}}{dI_N^{inc}} = F_0 e^{-\frac{1}{2}\tilde{q}^2}. \tag{24}$$

and, according to equations (6) and (7) reduces to unity outside the cone of coherence.

5. Contribution from the central laser photons ($\theta_L = 0$)

To understand what the situation would be like in a real experiment, one has to add up the contributions (equation 23) over all possible values of ℓ and m. It is illustrative to consider the contribution that comes from the solid angle

$$\Delta\Omega = 4\pi \sin^2 \tfrac{1}{2} \Delta\theta_L \tag{25}$$

concentrated in a small angular region around the direction $\theta_L = 0$, where the formalism just described appreciably simplifies. In this direction, following the Appendix, the form factor of equation (17) becomes

$$|F_0|^2 \equiv |F(\mathbf{q}, \theta_L \cong 0)|^2 \cong N_e^2 \frac{\xi^2 \eta^2}{(\xi^2 + \sigma_y^2)(\eta^2 + \gamma^2 \sigma_z^2)} e^{-\left(\frac{\beta c t}{\sigma_z}\right)^2} e^{-\frac{1}{2}\left(\frac{q_x^2}{u^2} + \frac{q_y^2}{v^2} + \frac{q_z^2}{f^2}\right)}. \tag{26}$$

Aside from the trivial case $q_x = q_y = q_z = 0$, this expression is strongly peaked at the values

$$q_x = q_y = 0, \qquad q_z = -2\beta\gamma k_L, \tag{27}$$

and in practice vanishes everywhere else. Therefore, it describes a photon pulse of length $\sigma_z/\sqrt{2}\beta$ that propagates (in the ERF) along the direction specified by equation (16) for $\theta_L = 0$

$$\cos\theta = \frac{1}{\gamma}, \qquad \phi = \frac{\pi}{2}. \tag{28}$$

According to equation (27), the x- and y-components of the momentum remain unchanged and the z-component changes sign. This means that the direction where the coherence builds up is obtained by reflecting the direction of the incoming photon momentum on a plane perpendicular to the z-axis. Going back to equation (23), the integration over the solid angle yields

$$\int_{4\pi} e^{-\frac{1}{2}\left(\frac{q_x^2}{u^2} + \frac{q_y^2}{v^2} + \frac{q_z^2}{f^2}\right)} d\Omega = e^{-\frac{q_z^2}{2f^2}} \left(\sqrt{2\pi}\,\frac{u}{q_z}\right)\left(\sqrt{2\pi}\,\frac{v}{q_z}\right). \tag{29}$$

Let us now integrate equation (23) over the region (equation 25) and then over time. With the definition of α of equation (10), one obtains the total number of photons coherently generated by the collision of the whole electron pulse against the laser photons, selected in the cone defined by equation (25)

$$N_{ph}^{coh} = \frac{\sigma_{Th}}{\sqrt{\pi}} \frac{W\gamma k_L^2}{\hbar\omega} \left(N_e \frac{\xi\eta}{\sqrt{\xi^2 + \sigma_y^2}\sqrt{\eta^2 + \gamma^2\sigma_z^2}}\right)^2 \sin^2 \frac{1}{2} \Delta\theta_L \left(\frac{uv}{q_z^2}\right) e^{-\frac{q_z^2}{2f^2}} \frac{\sigma_z}{\beta c}. \tag{30}$$

This expression validates the simple interpretation that all the electrons confined in the illuminated area radiate in phase, and hence the emitted radiation adds up as the square of their number. The obtained intensity is determined by the Thomson cross section and is confined to the diffraction limited solid angle

$$2\pi \frac{uv}{q_z^2} = \frac{1}{16\pi\beta^2} \frac{(\lambda_L/\gamma)^2}{\sigma_x \sigma_y} \frac{\sqrt{\xi^2 + \sigma_y^2}}{\xi} \tag{31}$$

along the direction defined by equation (28).

The total number of photons that would be expected from a purely incoherent scattering and in the same solid angle is

$$N_{ph}^{inc} = \sqrt{\frac{2}{\pi}}\,\sigma_{Th}\,\frac{W\gamma k_L^2}{\hbar\omega}\,N_e\,\frac{\xi\eta}{\sqrt{\xi^2+\sigma_y^2}\sqrt{\eta^2+\gamma^2\sigma_z^2}}\,\sin^2\frac{1}{2}\,\Delta\theta_L\left(\frac{uv}{q_z^2}\right)\frac{\sigma_z}{\beta c} \tag{32}$$

and therefore the coherent/incoherent ratio at $\theta_L \cong 0$ becomes

$$\Re(\theta_L \cong 0) = \frac{N_e}{\sqrt{2}}\,\frac{\xi\eta}{\sqrt{\xi^2+\sigma_y^2}\sqrt{\eta^2+\gamma^2\sigma_z^2}}\,e^{-\left(4\pi\beta\frac{\eta}{\lambda_L}\right)^2}. \tag{33}$$

This ratio is an optimum when

$$\xi = \eta = \sigma_y = g\,\frac{\lambda_L}{2\pi}, \tag{34}$$

with $g(>1)$ a coefficient reflecting the difficulty of achieving in practice a diffracted limited laser beam.

In this case, because $\sigma_z = \gamma\sigma_{z,L}$, equation (33) reduces to

$$\Re(\theta_L \cong 0) = \frac{N_e}{\sigma_{z,L}}\left(\frac{\lambda_L}{4\gamma^2}\right)\frac{1}{\pi}\,ge^{-4g^2\beta^2}. \tag{35}$$

Equation (35) explicitly shows that the coherent enhancement is proportional to the linear density of electrons in the bunch and to the scattered wavelength $\lambda_L/4\gamma^2$. Equation (33) also shows that $\Re$ strongly depends on the ratio between laser waist and wavelength.

6. Numerical estimates

We are now in the position to work out some crude numerical estimates of the expected rates. Let us assume, for argument's sake, to have an electron bunch with the following features (Villa 1988)

$$\begin{aligned} &N = 5.10^{11}, \qquad \varepsilon = 10^{-7}\ \text{m} - \text{rad}, \qquad \sigma_{z,L} = 3\ \text{mm (10 ps)} \\ &E = 7.47\ \text{MeV}, \qquad \gamma = 14.6 \end{aligned} \tag{36}$$

and a Nd:YAG laser pulse (1.06 μm) of 10 mJ/100 ps focused to a spot size

$$\xi = \eta = g\,\frac{\lambda_L}{2\pi} = 0.21\ \mu\text{m}, \quad (g = 1.2). \tag{37}$$

With the emittance value quoted in equation (36), it should be possible also to focus the electron beam to the same spot size. The coherent enhancement, from equation (35) results

$$\Re = 249.$$

The contribution that comes from the central region of the beam (equation 25) with $\Delta\theta_L = 10°$ corresponds to a total yield of 5×10^6 coherent photons per pulse (equation 30), concentrated in a solid angle of 2.7×10^{-4} sterad (equation 31), and centered around the direction $\theta = 87.1°$, $\phi = 90°$ (equation 28), practically parallel to the electron beam, in the ERF system. This means that if the repetition rate is of the order of 1 KHz, one can have (in the LAB) 1 keV highly collimated coherent photons at the rate of 5×10^9/s.

Equation (35) shows that the number of electrons that contribute to coherent emission is, in this example

$$N_e \frac{\lambda}{\sigma_{z,L}} = 2.3 \times 10^5,$$

with $\lambda = \lambda_L/2\gamma^2$ the scattered photons' wavelength. A g-dependent form factor

$$\frac{1}{\pi} g e^{-4g^2\beta^2}$$

critically determines the actual coherent yield.

7. Conclusion

We claim that coherent effects arise in Compton scattering at large angles (in particular, at 90°), when the laser beam is strongly focused on the electron trajectory and the electron density is sufficiently high. These conditions can be achieved with present-day lasers and electron high-gradient, low-emittance linacs (Villa 1988, 1990). In particular, we have demonstrated that the central part of the laser beam generates a coherent beam of photons in a narrow cone very well defined in the ERF system, with an intensity several hundred times higher than the corresponding incoherent yield. This coherent radiation propagates in the LAB practically along the electron beam direction and can be easily selected with a suitable collimator.

Moreover, also in the case when one is not interested in the coherence properties of the radiation, collective effects will enhance the scattering yield, in comparison with the ordinary backscattering case.

Finally, one has to bear in mind that a complete picture of the radiation pattern can only be obtained by a numerical study of the form factor integral appearing in equation (23), with similar techniques as used to calculate the incoherent backscattered intensity (Tang *et al.* 1993a,b).

REFERENCES

Bénard, C. & Rousseau, M. 1974 *J. Opt. Soc. Am.* **64**, 1433.

Federici, L. *et al.* 1980 *Nuovo Cimento* **59B**, 247.

Ginzburg, I.F. *et al.* 1983a *Nucl. Inst. Methods* **205**, 47.

Ginzburg, I.F. *et al.* 1983b *Sov. J. Nucl. Phys.* **38**, 222.

Jackson, J.D. 1975 *Classical. Electrodynamics*, 2nd ed., (John Wiley, New York), p. 417. (In this reference, the form factor is defined as the absolute-squared of our F.)

Kim, K.J. *et al.* 1992 Lawrence Berkeley Laboratory Report LBL-33074.

Kim, K.J. *et al.* 1994 *Nucl. Inst. Meth.* **341**, 351.

Lipkin, H.J. 1987 *Phys. Rev. Lett.* **58**, 1176.

Luccio, A. *et al.* 1990 *Laser Part. Beams* **8**, 383.

Luccio, A. & Miceli, L. 1994 *J. X-Ray Sci.* **4**, 247.

Pellegrini, C. 1982 In *Conference on New Horizons in Electromagnetic Physics* (Charlottesville, VA).

Sandorfi, A.M. *et al.* 1983 *IEEE Trans. Nucl. Sci.* **NS-30**, 3083.

Tang, C-M. *et al.* 1993a *Nucl. Inst. Meth.* **331**, 371.

Tang, C-M. *et al.* 1993b Naval. Research Laboratory Report NRL/MR/6791-93-7328.

Villa, F. 1988 *Proc. Switched Power Workshop.*

Villa, F. 1990 U.S. Patent 4975917.

Weber, J. 1985 *Phys. Rev. C* **31**, 1468.

APPENDIX

With the following positions

$$A = \frac{1}{2}\left[\frac{1}{\sigma_x^2} + \tan^2\theta_L\left(\frac{\cos^2\phi_L}{\xi^2} + \frac{\sin^2\phi_L}{\eta^2}\right)\right], \qquad E = -\gamma\,\frac{\tan\theta_L \sin\phi_L}{\eta^2}$$

$$B = \frac{1}{2}\left(\frac{1}{\sigma_y^2} + \frac{1}{\xi^2}\right), \qquad F = \gamma^2\,\frac{\beta c}{\eta^2},$$

$$C = \frac{1}{2}\left(\frac{1}{\sigma_z^2} + \frac{\gamma^2}{\eta^2}\right), \qquad G = \beta c E, \tag{A.1}$$

$$D = -\frac{\tan\theta_L \cos\phi_L}{\xi^2}, \qquad H = \frac{(\gamma\beta c)^2}{2\eta^2},$$

the integral of equation (14) of the text becomes

$$F(\mathbf{q}) = \frac{1}{(2\pi)^{3/2}}\,\frac{N}{\sigma_x\sigma_y\sigma_z}\iiint_{-\infty,+\infty} e^{-P(x,y,z)}e^{i\mathbf{q}\cdot\mathbf{r}}\,dx\,dy\,dz,$$

$$P(x,y,z) = Ax^2 + By^2 + Cz^2 + Dxy + Exz + Fzt + Gxt + Ht^2, \tag{A.2}$$

$$\mathbf{q}\cdot\mathbf{r} = q_x x + q_y y + q_z z.$$

The quadratic form appearing in this expression can easily be diagonalized with the linear transformation

$$x' = ux + ly + mz, \qquad y' = fz, \qquad z' = vy + \omega z, \tag{A.3}$$

where

$$u = \sqrt{A}, \qquad l = \frac{D}{2\sqrt{A}}, \qquad m = \frac{E}{2\sqrt{A}}, \qquad v = \sqrt{B - \frac{D^2}{4A}},$$

$$f = \sqrt{C - \frac{E^2}{4A} - \frac{(DE)^2}{16A^2v^2}}, \qquad \omega = -\frac{DE}{4Av}, \tag{A.4}$$

and one has

$$P(x,y,z) = (x_0 + x')^2 + (y_0 + y')^2 + (z_0 + z')^2 + (x_0^2 + y_0^2 + z_0^2), \tag{A.5}$$

where

$$x_0 = \frac{Gt}{2u}, \qquad y_0 = \frac{Ft}{2f} + \frac{l\omega - vm}{2uvf}\,Gt, \qquad z_0 = -\frac{l}{2uv}\,Gt. \tag{A.6}$$

The integral of equation (14) is thus reduced to the form

$$F(\mathbf{q}) = \frac{1}{(2\pi)^{3/2}}\,\frac{N}{\sigma_x\sigma_y\sigma_z}\,e^{(|\mathbf{r}_0|^2 - Ht^2)}\iiint_{-\infty,+\infty} e^{-|\mathbf{r}'+\mathbf{r}_0|^2}e^{i\tilde{\mathbf{q}}\cdot\mathbf{r}'}\left|\frac{\partial(x,y,z)}{\partial(x',y',z')}\right| dx\,dy\,dz,$$

$$\mathbf{r}_0 \equiv (x_0, y_0, z_0), \qquad \mathbf{r}' \equiv (x', y', z'), \tag{A.7}$$

$$\tilde{q}_x = \frac{q_x}{u}, \qquad \tilde{q}_y = \frac{l\omega - vm}{uvf}\,q_x - \frac{\omega}{vf}\,q_y + \frac{1}{f}\,q_z, \quad \tilde{q}_z = \frac{1}{v}\,q_y - \frac{l}{uv}\,q_x.$$

Because the Jacobian of the linear transformation equation (A.3) is

$$\frac{\partial(x,y,z)}{\partial(x',y',z')} = \frac{1}{uvf}, \tag{A.8}$$

equation (A.7) becomes

$$F(\mathbf{q}) = \frac{1}{2^{3/2}} \frac{N}{\sigma_x \sigma_y \sigma_z} \frac{1}{uvf} e^{(|\mathbf{r}_0|^2 - Ht^2)} e^{-i\tilde{\mathbf{q}}\cdot\mathbf{r}_0} e^{-\frac{1}{4}\tilde{q}^2} = F_0 e^{-i\tilde{\mathbf{q}}\cdot\mathbf{r}_0} e^{-\frac{1}{4}\tilde{q}^2}, \tag{A.9}$$

which coincides with equation (18) of the text.